American Journal of Civil Engineering and Architecture, 2016, Vol. 4, No. 4, 125-132
Available online at http://pubs.sciepub.com/ajcea/4/4/3

DOI:10.12691/ajcea-4-4-3

Estimation of the Yield Stress of Cement Pastes from Electrical Resistivity Measurement

Mbujje Joel Webster[1,*], Wei XiaoSheng[1], Makorogo Javilla Barugahare[2]

[1]School of Civil Engineering and Mechanics, Huazhong University of Science and Technology, 430074, Wuhan, China
[2]State Key Laboratory of Silicate, Wuhan University of Technology, 430070, Wuhan, China
*Corresponding author: mbujje@gmail.com

Abstract This study proposes a continuous method for predicting the yield stress development from mixing until the final setting point. Samples prepared with water to cement ratios (w/c) of 0.3, 0.35 and 0.4 are tested using a vane in cup rheometer, a Vicat needle and a non contact electrical resistivity machine (NC-ERM). Times corresponding to the initial yield stress (ta), a dramatic increase in the yield stress (tb), a maximum torque reading on the rheometer (tc), an initial setting (td) and a final setting (te) on the yield stress-time ($\tau(t)$-t) curve are correlated with the time at a point of inflexion (tP) on the bulk resistivity-time ($\rho(t)$-t) curve. A quantitative relationship developed between the yield stress and electrical resistivity shows a good agreement with experimental data.

Keywords: *electrical resistivity, yield stress, cement paste, water to binder ratio*

Cite This Article: Mbujje Joel Webster, Wei XiaoSheng, and Makorogo Javilla Barugahare, "Estimation of the Yield Stress of Cement Pastes from Electrical Resistivity Measurement." *American Journal of Civil Engineering and Architecture*, vol. 4, no. 4 (2016): 125-132. doi: 10.12691/ajcea-4-4-3.

1. Introduction and Methodology

1.1. Introduction

There is a need for the continuous quality control of workmanship and materials at a modern construction site. The performance of concrete during pumping, spreading, molding and compaction can be inferred from the yield stress of a cement paste behavior before hardening [1]. The yield stress of cement pastes in a very fluid state has been evaluated by mini slump cone [2,3,4,5], marsh cone [6,7,8,9] and rheometers [10,11,12]. Recent researches have shown that there is a relationship between setting time as determined empirically by a Vicat needle and shear yield stress [13,14,15], Liao et al [16] has gone ahead to determine the yield stress at initial setting time and final setting time as 32.4kPa and 780kPa respectively [16].

The mini slump cone, Vicat needle and marsh cone are relatively available, affordable and require less skilled labor to operate in comparison with a rheometer. However, all methods discussed require several discrete measurements on the sample to gain an understanding of the development of yield stress with the time. Furthermore, rheometers of different configuration report different values of the yield stress even for the same sample, although the trend of change may be similar [17]. The limited range of the rheometers and insensitivity of the Vicat apparatus at a low yield stress (<18kPa) has been highlighted by the reference [18].

The objective of this study is to propose an alternative method based on the electrical resistivity to evaluate a yield stress of cement pastes over a wider range of fluidity than the methods discussed earlier. We utilized a Non Contacting Electrical Resistivity Machine (NC-ERM) that was invented by Li and Li [19] and manufactured by Hong Kong Brilliant Concept Technologies. Liu et al [20] and Wei et al [21,22] have previously used the apparatus successfully that used to study the hydration of cementiteous materials [20,21,22]. It overcomes major draw backs of an alternative electrical resistivity apparatus such as polarization due to DC currents and a poor contact between the sample and probes. The machine consists of a transformer that generates a voltage across the primary coil. This induces a voltage across the sample (secondary coil). The current across the sample is measured by a current meter and resistivity of cement sample computed from Ohms law.

1.2. Methodology

The typical yield stress and an electrical resistivity development with time curves are shown in Figure 1(a) and Figure 1(b), respectively. From Figure 1(a), the general development of the yield stress with time is a four stage process separated by characteristic points B, C and D. The yield stress in the stages AB, BC, and CD has been shown to be linear [18]. For the case of this study, a linear growth of the shear yield stress is assumed between the torque limit of the rheometer and the initial setting, D due to lack of a suitable apparatus to measure its evolution. In the stage DE, a yield stress from Vicat needle penetration has been shown to fit a parabolic curve [16]. The evolution of a yield stress of cement pastes is largely affected by a porosity reduction which is reflected by a three dimensional network that often forms due to flocculation [23]. Similarly, the reduction in porosity results in an increase in resistivity between points M and P as shown in Figure 1(b). This period has been understood to include the dormant and acceleration stages of hydration [24,25,26].

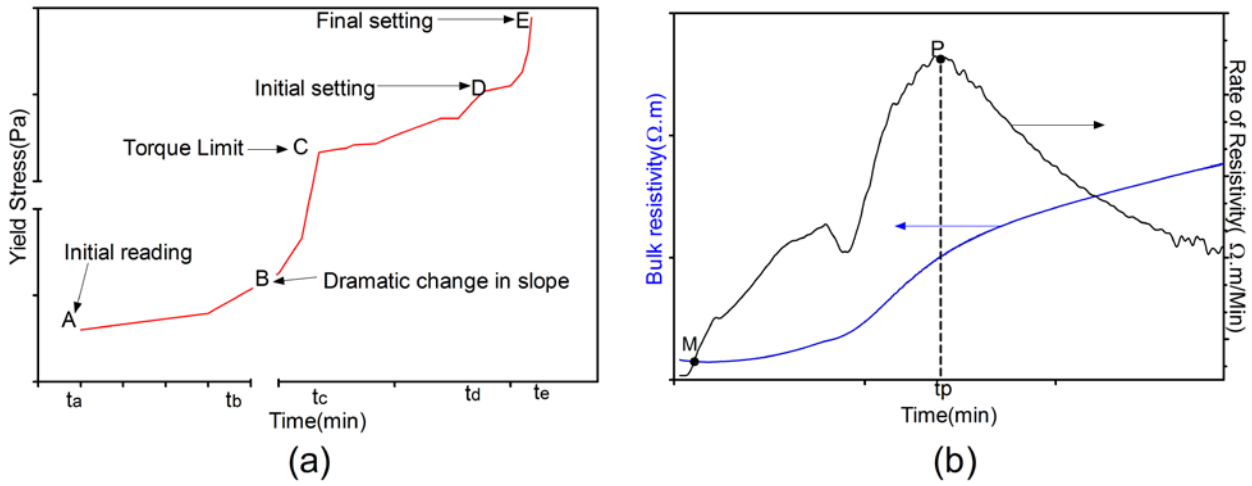

Figure 1. Typical development with time of (a) yield stress (b) electrical resistivity and rate of resistivity

It is upon this background that a relationship between the yield stress and the electrical resistivity is formulated as illustrated in Figure 2 and computed according to the following steps:

Step 1: The critical times from the yield stress curve are expressed as a function (g) of time, tp from the resistivity curve by a linear regression as expressed in Eq. (1).

Step 2: From the equation of τ (t) obtained from τ (t)-t and the relationship between yield stress critical times and tp from the resistivity curve, yield stress is expressed in terms of tp.

Step 3: The influence of water to cement ratio (w/c) is incorporated and the general equation is given by Eq. (2).

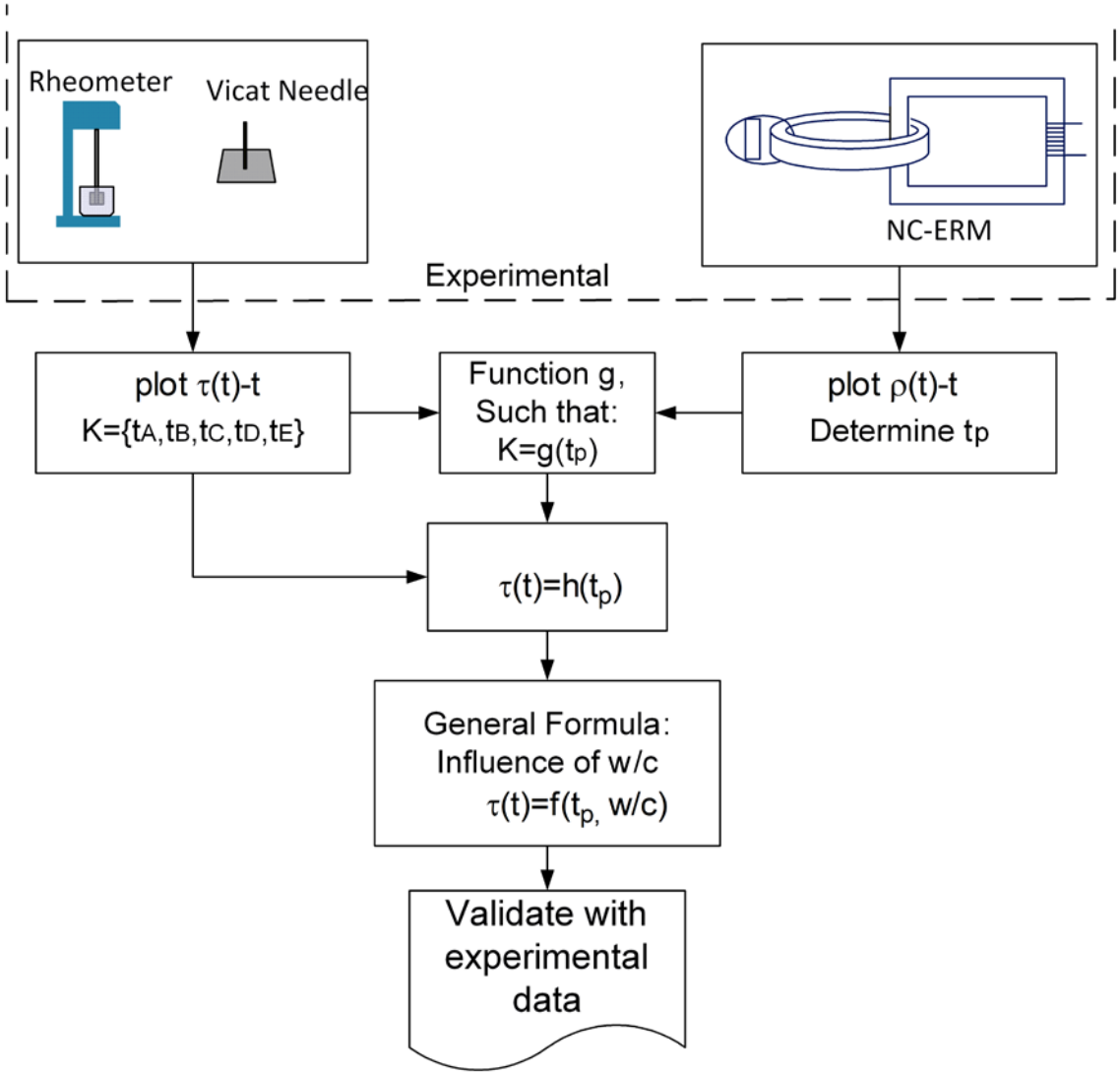

Figure 2. Algorithm to predict yield stress from electrical resistivity

2. Materials and Samples Preparation

2.1. Materials

P·O 42.5 that meets the requirements of Chinese cement standard GB/T17671-1999 was used for this study. Its chemical properties are shown in Table 1. Distilled water was used throughout the experiment.

Table 1. Chemical compositions of cement.

Oxide	CaO	SiO_2	Al_2O_3	Fe_2O_3	MgO	SO_3	Na_2O	K_2O	LOI
Weight(%)	63.02	21.88	4.02	2.59	2.44	3.10	0.32	0.15	1.68

2.2. Samples Preparation

Pastes for all the three experiments were mixed using a planetary mixer in the laboratory. The mixing program consisted of a slow mixing at 45 rpm for 120 seconds followed by a fast mixing at 90 rpm for a further another 120 seconds. There was a 15 seconds interval between the two mixing regimes to allow for cleaning. The samples are mixed with water to cement ratios (w/c) of 0.3, 0.35 and 0.4 and labeled as W 0.3, W 0.35 and W 0.4, respectively.

3. Experimental

3.1. Rheology

A vane in cup rheometer (Brookfield SST 2000) was used to monitor the stress growth with time. After mixing in the planetary mixer, samples were prepared in glass cylinders and pre-sheared at 150 Pa for 60 seconds to establish the uniform microstructure. The vane used had a diameter of 15 mm and height of 30 mm and the gap between the vane and the walls of the cylinder was 10 mm. The temperature in the room was maintained at 200°C using an air conditioner and all samples were covered with a moist cloth to prevent evaporation. To determine the yield stress after a period of time, a constant shear rate of 0.01S-1 was applied [27] and the yield stress is determined as the maximum shear stress on the shear stress-time plot [28].

3.2. Vicat Needle

The test was performed according to ASTM C191. In this paper, however, the cement paste was not of standard consistency but of water to cement ratios 0.3, 0.35 and 0.4 as required for all the other tests on the yield stress and the electrical resistivity [29].

3.3. Electrical Resistivity

The apparatus used is illustrated in Figure 3. Each sample is placed in a plastic mold and tested up to 24 hours using a procedure adopted by Xiao et al [26]. Each sample is prepared in the same way as the one used for the rheological measurement and the Vicat penetration. Data points are collected continuously every minute and recorded by a computer. The method is versatile for its ability to continuously monitor the cement paste hydration without having to destroy the bonds that are formed.

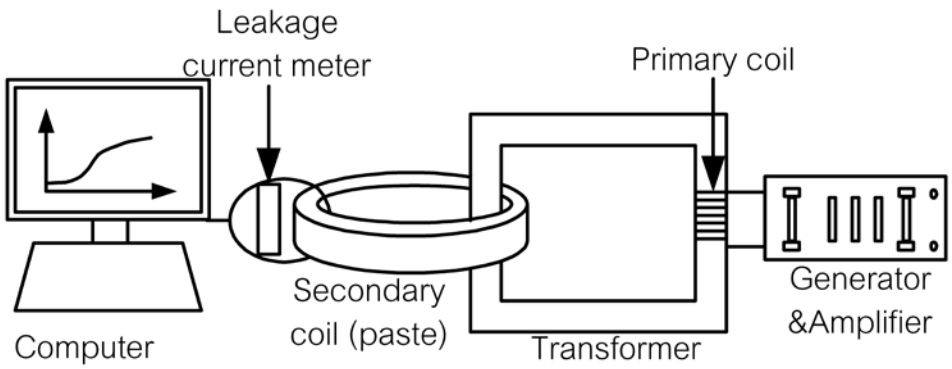

Figure 3. Schematic of Non Contacting Electrical Resistivity Machine (NC-ERM)

Table 2. Critical points from rheology, vicat needle and Resistivity measurements.

Sample	Rheology						Vicat Needle		Resistivity	
	(min)			(Pa)			(min)		(min)	
	t_a	t_b	t_c	τ_a	τ_b	τ_c	t_d	t_e	t_m	t_p
W0.3	10	86	150	284	900	4350	197	318	90	536
W0.35	10	118	180	96	880	4350	277	372	95	559
W0.4	10	149	210	52	850	4350	294	435	105	691

4. Results and Discussions

A summary of all the critical points from the rheometer, Vicat needle and the resistivity measurements is presented in Table 2.

4.1. Rheological Measurements

Figure 4 shows the typical change of the shear stress development with strain at a constant shear rate of 0.01S-1 for sample W 0.3 at a time of 90 minutes. The shear stress

rises steadily to a maximum value of 1131 Pa before dropping rapidly. This agrees with what is expected from the operation manual for slurries such as cement paste [28], where the shear stress rises to yield stress and drops thereafter due to the microstructure breaks down. The yield stresses obtained at intervals of 30 minutes are plotted against the hydration time in Figure 5. It is interesting to note that the abrupt change in a slope at point B occurs at approximately the same yield stress for all the samples (~900Pa). In the stage AB, the rate of gain of the shear resistance is of 1 order of magnitude but quickly changes to an order of 10 in the stage BC for all the samples as listed in Table 3. The change in the rate of gain of shear resistance at the point B has been interpreted to be the onset of setting [18,30].

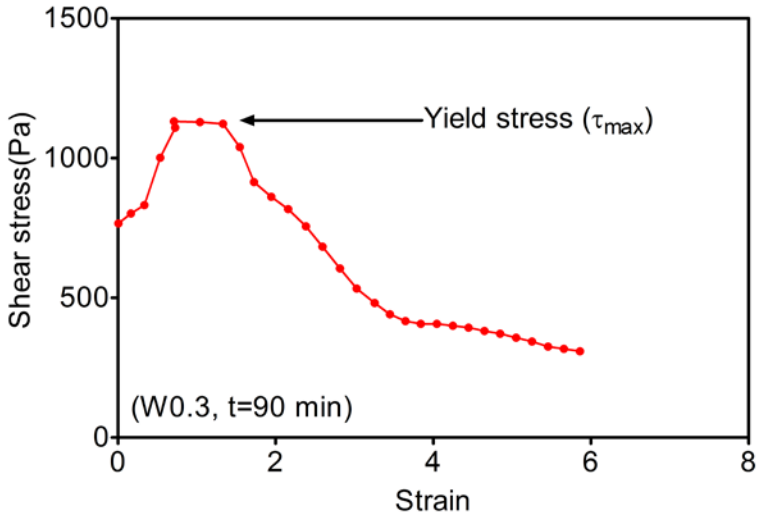

Figure 4. Typical shear stress with time (w/c=0.3, t=90 min)

Table 3. Analysis of yield stress curve for all samples

Sample	Rate of gain of stress (Pa/min)			n			L
	AB	BC	CD	AB	BC	CD	DE
W0.3	8.1	53.9	596.8	-3735	596.8	-85171	7.5
W0.35	7.25	56.0	289.1	-5724	289.1	-47702	10.1
W0.4	5.741	57.37	329	-7699	329	-63357	11.56

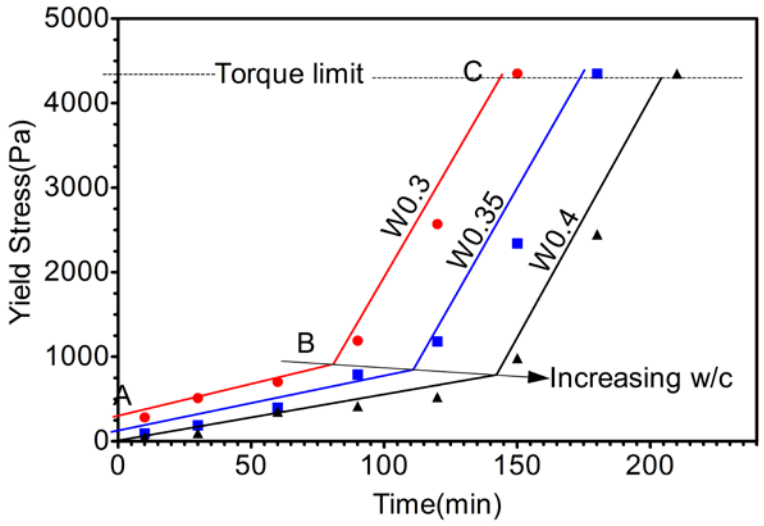

Figure 5. Yield stress against time from a rheometer

The water to cement ratio has a pronounced effect on the occurrence of characteristic points B and C as depicted in Figure 5. Samples prepared with a w/c of 0.4 (W 0.4) hydrated for the longest time before the drastic change in the rate of stress development. The point B for the sample W 0.4 occurred at 149 min, and 31 minutes is longer than W 0.35 and 63 minutes and later than the W 0.3. This is an indication of delay in strength development with water fraction which is consistent with cement chemistry. Roussel et al [31] discussed the forces that could be responsible for the development of the yield stress in cement paste namely; colloidal interactions, Brownian forces, and hydrodynamic forces and other contact forces. However, of these, the gain of permanent shear resistance was demonstrated to be a consequence of hydration [32]. Thus, the delay in occurrence of points B and C in Figure 5 indicates a lower degree of hydration in samples with a higher water to cement ratio.

4.2. Vicat Results

Figure 6 shows the typical depth of penetration of the Vicat needle with time for sample W 0.3. It can clearly be seen that the penetration is 40 mm from initial time of mixing until 135 minutes when it begins to decreasing with time. Figure 7 illustrates the development of yield stress which is computed from the penetration depth using Eq. (3) that was adopted by Liao et al [16]. This points out that the depth of penetration reduces with the increase in the shear resistance.

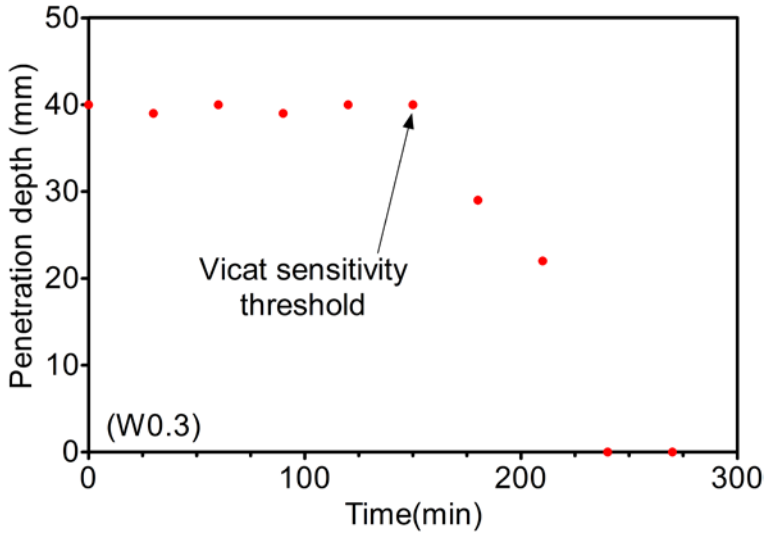

Figure 6. Depth of penetration with time (w/c=0.3)

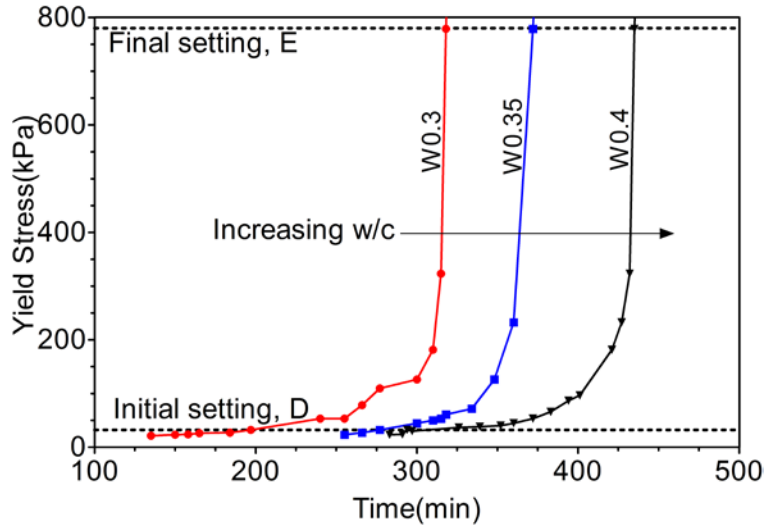

Figure 7. Yield stress with time from vicat needle penetration

Where: m is the mass of the needle (300 grams), g is the acceleration due to gravity, r is the radius of the needle (0.565 mm) and h is the depth of penetration.

Furthermore, the yield stress at the sensitivity threshold of the Vicat needle is 20 kPa from Eq. (3). Consequently not until the cement paste can develop the shear resistance of 20 kPa, will the Vicat needle measure resistance to penetration. This explains the complete penetration of the needle for over two hours after mixing in Figure 6. The curves of best fit in the stage DE for the development of the yield stress with time in Figure 7 can be approximated to a parabolic curve with a variable L. It is dependent on water to cement ratio as shown in Eq. (4) and listed in Table 3.

The initial setting (td) and final setting times (te) are sensitive to the water cement ratio as expected. Points D and E are seen in Figure 7 to shift right with an increase in w/c ratio. This is probably due to the increased pore space for the larger water particle in comparison with the cement particle. The larger inter-particle spaces need to be filled by hydration products before the paste is dense enough to support load.

More pertinent to this study, the initial setting time as indicated by the sharp change in gradient at the point B, tb (Figure 5) occurs more than 60 minutes earlier than initial setting time as detected by the Vicat needle (Figure 7). This is consistent with work by reference [30], who put forward the greater sensitivity of the rheometer as the reason for divergence in values reported by the two apparatus.

4.3. Resistivity

The bulk electrical resistivity development curve with time (is shown in Figure 8 and its differential curve (which represents the rate of resistivity development is shown in Figure 9. The minimum point, M and the inflection point P are marked on Figure 8 and Figure 9,

respectively. The characteristic time, tp at which the peak occurred for all the samples is listed in Table 2. More detail on how to determine critical points is shown in a research by Xiao et al [33]. From the Figure 9, it is observed that from M onwards, the resistivity increases with time for all samples considered. All the electrical development curves are S shaped, having an initial resistivity of about 1 ohm. m which reduces to a minimum value in the same order at the point M. However, from the point M towards the point P, the resistivity increases rapidly as demonstrated by the rate of the resistivity curve in Figure 9. Beyond P, the resistivity continues to increase indefinitely but at a reducing rate and the curves can be approximated to a parabolic curve. The difference in resistivity is more pronounced as the time increases. For instance, there is barely a noticeable difference in resistivity at the point M. However, at the point P the difference is all too pronounced.

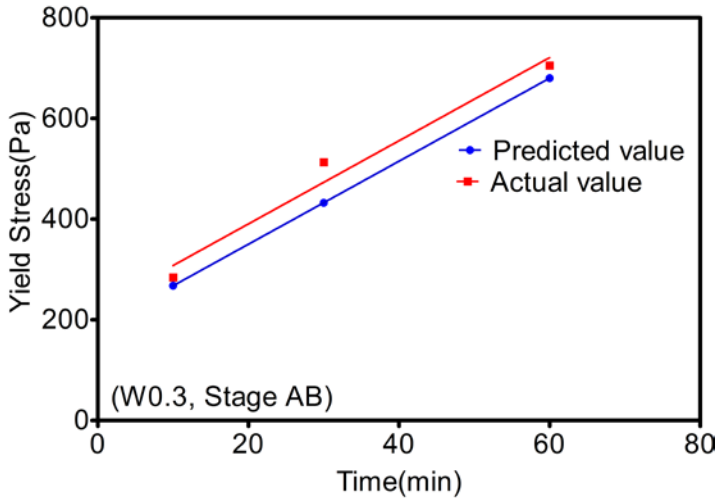

Figure 8. Electrical resistivity development with time for different cement pastes

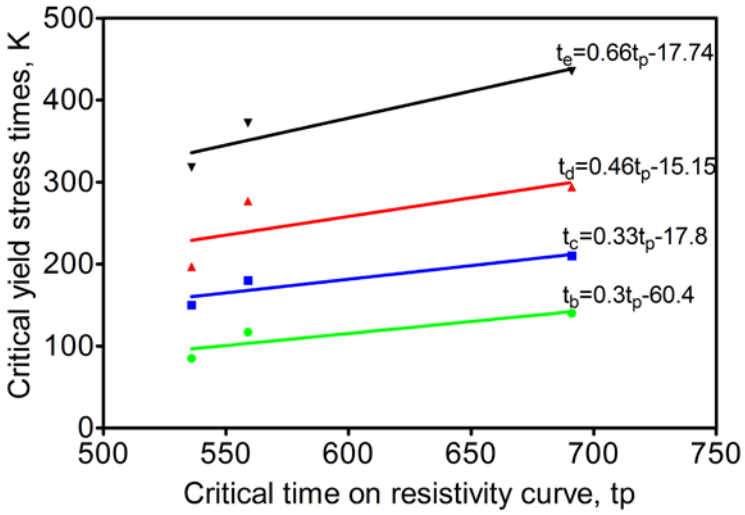

Figure 9. Rate of Resistivity development with time for different cement pastes

By considering the development of the resistivity as a time series, the time tp is seen to have a close relationship with the water to cement ratio; tp considerably lags with an increase of the w/c. Li et al [34] used similar apparatus [34] and showed a compelling evidence to suggest that the lag in the electrical resistivity and rate of resistivity development lends itself to the porosity reduction tha is revealed by the reduced gel/space ratio, they went on to show that the time between points M and P as pointed out on Figure 9 consists of the dormant and acceleration phase of the hydration process.

4.4. Relationship between Electrical Resistivity and Yield Stress

Figure 5 and Figure 7 exhibit a delay in the yield stress with an increase in w/c. Similarly, Figure 8 reveals a lag in the point P on the resistivity-time curve. By looking at the influence of w/c on the yield stress and electrical resistivity, the relationship between the critical time tp and the yield stress characteristic times K is proposed in Figure 10. It is evident that there exists a linear relationship between K and tp at all measurements taken and as such it can be deduced that both K and tp are clearly affected by the w/c. This relationship lays a framework upon which the yield stress is characterized from the electrical resistivity based on the assumption that the major factor affecting both is the porosity development.

By breaking down the development of yield stress into the time domain and w/c ratio domains, the yield stress is given out as a function of time and w/c ratio as shown in Eq. (5). Generally speaking, the yield stress and electrical resistivity reduce with w/c and increase with time.

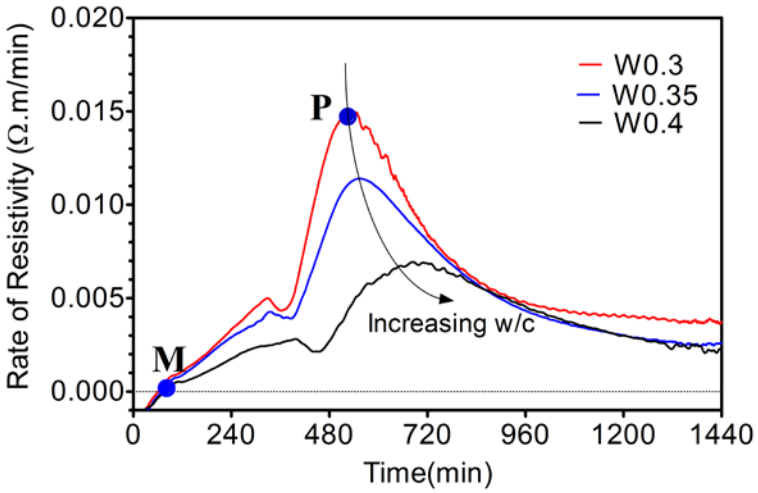

Figure 10. Linear regression of yield stress critical times, K with t_p

Furthermore, the contribution of porosity to the yield stress can be explained by packing density. For instance, the yield stress of W 0.3 at 10 minutes after mixing (284Pa) is 2.95 times that of W 0.35 and 5.46 times that of W 0.4. The solid volume fractions of cement paste, where and are the densities of cement and water, respectively. They are computed as 0.52, 0.48, and 0.45 for samples W 0.3, W 0.35 and W 0.4, respectively. This indicates a higher porosity for sample W 0.4 compared to W 0.3 thus a lower yield stress. Sak et al [35] and Bui et al [36] suggested that the proximity of the particles is responsible for stronger Van der waals forces in samples with lower water cement ratio [35,36]. This assertion is supported by the calculated solid volume fraction of cement.

4.5. The Validation of a Mathematical Model

A robust non contact electrical resistivity method has been employed to monitor the cement paste hydration and correlate d with a yield stress measured by a Vicat needle and a vane in cup rheometer (Brookfield SST 2000). The effects of water to cement ratio and time are examined and modeled in Eq. (5).

The model suggested in Eq. (5) is validated with data for a sample of w/c=0.3 during the stage AB at t=10, 30 and 60 minutes. It is seen that the predicted values are within 5 % of the measured values as shown in Figure 11. The yield stress can be reliably predicted from an electrical resistivity using the time corresponding to the peak point P.

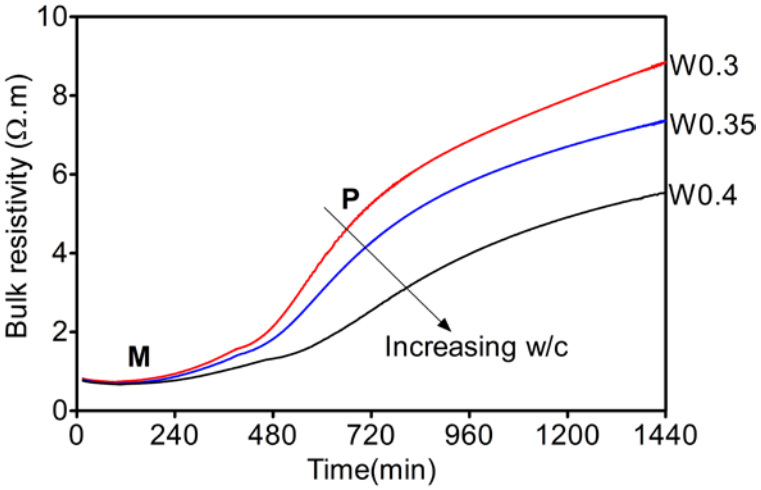

Figure 11. Validation of model in the stage AB (w/c=0.3)

5. Conclusions

Within the experimental range, the findings of this study are as follows:

(1) The increase in w/c ratio delays both the yield stress and the electrical resistivity development with time. This can be attributed to the increased porosity that affects both yield stress and electrical resistivity of cement pastes.

(2) The linear relationship between the yield stress critical times, K and the characteristic time, tp on the resistivity curve is a further indication that both yield stress and electrical resistivity reduce with w/c and increase with time.

(3) The empirical relationship between the electrical resistivity development and the yield stress growth has been put forward and it shows a good agreement with experimental data.

(4) The method suggested in this study has the potential to evaluate the yield stress from mixing until the final setting time. This makes it more applicable over a wide range of fluidity than the mini slump cone, marsh cone, Vicat needle and most available rheometers.

Acknowledgement

The authors wish to express their gratitude and sincere appreciation to the National Natural Science Foundation of China (51478200).

References

[1] Banfill, P., *Rheology of fresh cement and concrete.* Rheology reviews, 2006. 2006: p. 61.

[2] Roussel, N., C. Stefani, and R. Leroy, *From mini-cone test to Abrams cone test: measurement of cement-based materials yield stress using slump tests.* Cement and Concrete Research, 2005. 35(5): p. 817-822. 11.

[3] Bahurudeen, A., et al., Development of sugarcane bagasse ash based Portland pozzolana cement and evaluation of compatibility with superplasticizers. Construction and Building Materials, 2014. 68: p. 465-475.

[4] Baldino, N., et al., Rheological behaviour of fresh cement pastes: Influence of synthetic zeolites, limestone and silica fume. Cement and Concrete Research, 2014. 63: p. 38-45.

[5] Bouvet, A., E. Ghorbel, and R. Bennacer, The mini-conical slump flow test: Analysis and numerical study. Cement and Concrete Research, 2010. 40(10): p. 1517-1523.

[6] Benaicha, M., et al., Marsh cone coupled to a plexiglas horizontal channel: Rheological characterization of cement grout. Flow Measurement and Instrumentation, 2015. 45: p. 234 126-134.

[7] Guria, C., R. Kumar, and P. Mishra, Rheological analysis of drilling fluid using Marsh Funnel. Journal of Petroleum Science and Engineering, 2013. 105: p. 62-69.

[8] Hallal, A., et al., Combined effect of mineral admixtures with superplasticizers on the fluidity of the blended cement paste. Construction and Building Materials, 2010. 24(8): p. 1418-1423.

[9] Jimma, B.E. and P.R. Rangaraju, Film-forming ability of flowable cement pastes and its application in mixture proportioning of pervious concrete. Construction and Building Materials, 2014. 71: p. 273-282.

[10] Ferraris, C.F., K.H. Obla, and R. Hill, The influence of mineral admixtures on the rheology of cement paste and concrete. Cement and concrete research, 2001. 31(2): p. 245 245-255.

[11] Williams, D.A., A.W. Saak, and H.M. Jennings, The influence of mixing on the rheology of fresh cement paste. Cement and Concrete Research, 1999. 29(9): p. 1491-1496.

[12] Cardoso, F.A., et al., Parallel-plate rotational rheometry of cement paste: Influence of the squeeze velocity during gap positioning. Cement and Concrete Research, 2015. 75: p. 250 66-74.

[13] Lootens, D., et al., Yield stress during setting of cement pastes from penetration tests. Cement and Concrete Research, 2009. 39(5): p. 401-408.

[14] Sleiman, H., A. Perrot, and S. Amziane, A new look at the measurement of cementitious paste setting by Vicat test. Cement and Concrete Research, 2010. 40(5): p. 681-686.

[15] Sonebi, M., M. Lachemi, and K.M.A. Hossain, Optimisation of rheological parameters and mechanical properties of superplasticised cement grouts containing metakaolin and viscosity modifying admixture. Construction and Building Materials, 2013. 38: p. 126-138.

[16] Liao, Y. and X. Wei, Penetration resistance and electrical resistivity of cement paste with superplasticizer. Materials and structures, 2014. 47(4): p. 563-570.

[17] Ferraris, C.F., Measurement of the rheological properties of high performance concrete: state of the art report. JOURNAL OF RESEARCH-NATIONAL INSTITUTE OF STANDARDS AND TECHNOLOGY, 1999. 104(5): p. 461-478.

[18] Amziane, S., Setting time determination of cementitious materials based on measurements of the hydraulic pressure variations. Cement and Concrete Research, 2006. 36(2): p. 295-304.

[19] Li, Z. and W. Li, Contactless, transformer-based measurement of the resistivity of materials. 2003, Google Patents.

[20] Liu, Z., et al., An analytical model for determining the relative electrical resistivity of cement paste and C–S–H gel. Construction and Building Materials, 2013. 48: p. 647-655.

[21] Wei, X., L. Xiao, and Z. Li, Prediction of standard compressive strength of cement by the electrical resistivity measurement. Construction and Building Materials, 2012. 31: p. 341-272 346.

[22] Xiao, L. and Z. Li, Early-age hydration of fresh concrete monitored by non-contact electrical resistivity measurement. Cement and Concrete Research, 2008. 38(3): p. 312-319.

[23] Struble, L.J. and W.-G. Lei, Rheological changes associated with setting of cement paste. Advanced Cement Based Materials, 1995. 2(6): p. 224-230.

[24] Bîrlea, N.-M.C. and E.N. Culea. Electrical methods for testing building and construction materials. in First International Conference for PhD students in Civil Engineering, CE-280 PhD. 2012.

[25] Villagrán Zaccardi, Y., et al., Influence of temperature and humidity on Portland cement mortar resistivity monitored with inner sensors. Materials and corrosion, 2009. 60(4): p. 283 294-299.

[26] Li, Z., X. Wei, and W. Li, Preliminary interpretation of Portland cement hydration process using resistivity measurements. ACI Materials Journal, 2003. 100 (3).

[27] Amziane, S. and C.F. Ferraris, Cementitious paste setting using rheological and pressure measurements. ACI materials journal, 2007. 104 (2).

[28] Brookfield. [cited 2015 10-September]; Available from: http://www.brookfieldengineering.com/download/files/RSBro.pdf.

[29] Bentz, D.P. and C.F. Ferraris, Rheology and setting of high volume fly ash mixtures Cement and Concrete Composites, 2010. 32(4): p. 265-270.

[30] Sant, G., C.F. Ferraris, and J. Weiss, Rheological properties of cement pastes: a discussion of structure formation and mechanical property development. Cement and concrete Research, 2008. 38(11): p. 1286-1296.

[31] Roussel, N., et al., Steady state flow of cement suspensions: A micromechanical state of the art. Cement and Concrete Research, 2010. 40(1): p. 77-84.

[32] Roussel, N. and F. Cussigh, Distinct-layer casting of SCC: The mechanical consequences of thixotropy. Cement and Concrete Research, 2008. 38 (5): p. 624-632.

[33] Xiao, L. and Z. Li, New understanding of cement hydration mechanism through electrical resistivity measurement and microstructure investigations. Journal of materials in civil engineering, 2009. 21(8): p. 368-373.

[34] Li, Z., Advanced concrete technology. 2011: John Wiley & Sons.

[35] Saak, A.W., Characterization and modeling of the rheology of cement paste: With applications toward self-flowing materials. 2000.

[36] Bui, D., J. Hu, and P. Stroeven, Particle size effect on the strength of rice husk ash blended gap-graded Portland cement concrete. Cement and concrete composites, 2005. 27(3): p. 357-366.